JMEPEG (2011) 20:1015–1022
DOI: 10.1007/s11665-010-9734-x

1059-9495/$19.00

Microstructure and Dry Sliding Wear Behavior of Mg-Y-Zn Alloy Modified by Laser Surface Melting

X.X. Lv, H.Y. Liu, Y.B. Wang, Y. Lu, G.Y. Li, and J. An

(Submitted December 24, 2009; in revised form July 10, 2010)

Mg-11Y-2.5Zn alloy was surface-melted using a 6.0 kW continuous wave CO_2 laser as a heat-generating source. X-ray diffractometer, laser optical microscopy, and Vickers hardness indentation were used to characterize the microstructure and hardness of the Mg-11Y-2.5Zn alloy. The results show that the microstructure in the laser-melted zone can be greatly refined and hardness is slightly improved. Dry sliding tests were performed on the as cast and laser surface-melted Mg-11Y-2.5Zn alloys using a pin-on-disk configuration. Coefficients of friction and wear rates were measured within a load range of 20-320 N at a sliding velocity of 0.785 m/s. Laser surface-melted Mg-11Y-2.5Zn alloy exhibited good wear resistance when compared with the as cast one under given applied load conditions, which has been explained by refining of the microstructure in the melted zone. Morphologies of worn surface on the as cast and laser surface-melted Mg-11Y-2.5Zn alloys were examined using scanning electron microscopy. Four wear mechanisms, namely abrasion, delamination, thermal softening, and melting, have operated.

Keywords friction and wear behavior, laser surface melting, magnesium alloy

1. Introduction

Among the light metallic materials, Mg and its alloys are of great interest to automotive and aerospace industries because of their low densities and high specific strength (Ref 1, 2). Despite the attractive range of mechanical properties, a relative low strength both at ambient temperature and at elevated temperature and poor resistance to wear and corrosion are a serious impediment against wide applications of Mg alloys like Al alloys. Further improvement of mechanical properties by unconventional processing technique and surface modification has been required to extend the application area of Mg alloys. Recently, Inoue et al. (Ref 3, 4) have reported that the Mg-Zn-Y ($Mg_{97}Zn_1Y_2$ rapidly solidified powder metallurgy) alloy has excellent mechanical properties such as high strength above 600 MPa and elongation of 5% at ambient temperature and excellent elevated-temperature yield strength of 510 MPa at 423 K. The excellent mechanical properties were achieved by warm extrusion of gas-atomized $Mg_{97}Zn_1Y_2$ powders and the strengthening mechanism was considered to be due to the hcp (2H)-Mg fine grain matrix of 100-200 nm in diameter with long period stacking order (LPSO) phase and the homogeneously dispersed $M_{24}Y_5$ fine particles of less than 10 nm in diameter. Furthermore, Matsuda et al. (Ref 5) have reported that the exact role of LPSO phase in strengthening is prevention of the growth of {10-12} deformation twin in Mg matrix. And it is confirmed that the LPSO phase can be prepared by conventional casting method, in whose unit cell six close-packed planes of the magnesium crystal with a stacking sequence of ABCBCB′ where A and B′ layers are significantly enriched by Zn and Y. In fact, the LPSO phase is identified as X-Mg_{12}YZn phase in the PDF file Card 36-1273 by the Joint Committee on Powder Diffraction Standards (Ref 6).

While magnesium alloys would normally not be candidates for bearings, sliding seals or gears, there are situations in which their surfaces could come into contact with other materials so as to make their friction and wear behavior of interest. In the absence of detailed studies on the wear mechanisms in magnesium alloys, AZ91 and its composites have been given first priority due to their leading roles in structural application (Ref 7, 8). Chen and Alpas (Ref 9) investigated dry sliding wear of AZ91 against a steel counterface using a pin-on-disk apparatus and revealed that a transition from mild to severe wear occurred was controlled by the contact surface temperature of the alloy. They also established a sliding wear map for AZ91, in which the mild wear regime consisted of two sub-wear regimes, namely an oxidational wear regime and a delamination wear regime; the severe wear regime comprised a severe plastic deformation wear regime and a melt wear regime.

Laser processing has now been established as an effective and reliable means of improving surface properties of materials at a competitive price with super properties as compared to its counterpart processes. A number of attempts have been made to improve the wear properties of AZ- and WE-type magnesium alloys using laser as a heat source (Ref 10, 11). The results obtained in these studies were very promising as compared to other conventional processes. The RS P/M Mg-Zn-Y alloy has remarkable properties such as high yield strength, reasonable ductility, rendering it and its composites promising candidate materials for lightweight structural applications including tribological situation. Though as-cast Mg-Zn-Y alloy with coarse grain size dose not exhibit super mechanical properties

X.X. Lv, H.Y. Liu, Y.B. Wang, Y. Lu, G.Y. Li, and **J. An**, Department of Materials Science and Engineering, Key Laboratory of Automobile Materials, Ministry of Education, Nanling Campus of Jilin University, Changchun 130025, People's Republic of China. Contact e-mail: anjian@jlu.edu.cn.

as the RS P/M one, it is still expected that refining of the microstructure using laser surface melting could improve the tribological properties. However, reports on effect of laser surface modification on Mg-Zn-Y alloys containing LPSO phase are rare and more efforts should be made to gain a better understanding of the microstructural evolution and wear properties involved, which is also helpful to providing reference data to the limited work available, and to understanding of tribological properties of rapidly solidified Mg-Zn-Y alloys. The main purpose of this article is to study the change in microstructure and wear behavior of laser surface melted Mg-11Y-2.5Zn alloy sliding against hard surface of steel under dry sliding condition.

2. Experimental Procedures

2.1 Materials

The testing material was a Mg-11Y-2.5Zn (in mass percentage) alloy. It was prepared by conventional casting method from high purity 99.9% Mg, 99.9% Zn, and Mg-21.5% Y alloy under a shielding gas of CO_2-0.05% SF_6. Zn and Y elements were added into the melt at the temperature of 750 °C, after about 5 min manual stirring to facilitate uniform distribution of Zn and Y elements, the melt was reheated to 775 °C and kept for 15 min, then poured into a steel die preheated at 100 °C to yield a cylindrical ingot of 40 mm in diameter and 110 mm in length.

2.2 Laser Melting Process

Laser surface melting was performed by a 6 kW continuous wave CO_2 laser processing system with 10.6 μm wavelength. Specimens of 40 mm in diameter × 20 mm length, machined from Mg-11Y-2.5Zn alloy ingot, were polished with 800 grit SiC paper, then washed with alcohol, air-dried, and sprayed with a layer of black carbon to enhance absorption of the laser prior to laser surface melting. The specimens were mounted on a computer-controlled XY stage. A continuous coaxial flow of high-purity argon was used to protect the surface of specimens during laser treatment. To avoid severe oxidation and excessively rough surface formed on the surfaces of specimens, the laser melting parameters were optimized to be: laser power: 2000 W; scan speed: 1700 mm/min; diameter of laser beam spot: 4 mm; track overlapping: 25%.

2.3 Microstructural Observation and Hardness Measurement

The microstructure of surface-melted alloy was observed using an OLS3000 confocal scanning laser microscope. The crystalline phases in Mg-11Y-2.5Zn alloy were characterized by a Rigaku x-ray diffractometer (XRD). The Vickers hardness was measured with a 25 g load on an indentation tester that gave reading to a 0.01 HV, each hardness value was obtained from an average of at least three test results. Thermal transformation in laser surface-melted Mg-11Y-2.5Zn alloy was examined by means of differential thermal analysis (DTA: SETSYS16/18, ETARAM machine).

2.4 Friction and Wear Testing

Friction and wear testing was conducted on a pin-on-disk-type machine. All friction and wear tests were carried out under dry sliding conditions at room temperature of 25 °C. Specimens of 6 mm × diameter × 12 mm length were machined from both laser surface-melted and as-cast Mg-11Y-2.5Zn alloys. About 100 μm thick material was removed off from the laser-treated surfaces of the pins to gain a flat surface and then they were polished to have a smooth surface roughness of 0.4 μm Ra for wear test. The coefficient of friction, μ, was calculated from the friction moment to an accuracy of 0.01 Nm (recorded for the signal from strain gauges mounted on the torque tube in testing machine) using the following formula:

$$\mu = \frac{M}{RN} \qquad \text{(Eq 1)}$$

where M is the friction moment, R the radius of wear track (0.03 m), and N the normal load.

Specimens were weighed on a single pan electrical balance that gave reading to a 0.1 mg before and after the wear test. The difference in weight of the three test pins before and after the experiment gave the average weight loss from a sliding distance of 376.8 m distance from which the average wear volume was calculated. The disk was 70 mm in diameter and made of high carbon chromium steel hardened to a hardness of 57 HRC, its flat surface was ground to a constant surface roughness of about 0.4 μm Ra. The disk rotational speed was kept constant at 0.785 ms^{-1} throughout the investigation. The worn surfaces of the wear pins were examined with a JSM-5600 scanning electron microscope.

3. Results and Discussion

3.1 Microstructure and Hardness

X-ray diffraction analysis of the surfaces of the untreated and laser-melted alloys, as shown in Fig. 1(a) and (b), indicated that both the alloys equally consisted of magnesium-rich phase (α-Mg) and $Mg_{12}YZn$ phase, and the intensity of $Mg_{12}YZn$ (108) peak for laser-melted alloy was enhanced relative to that of Mg (101) due to a preferential orientation effect resulting from the epitaxial growth from the substrate under the constrained growth condition. The grains tend to grow more or less perpendicularly to the solid-liquid interface. To have a direct observation on the change in microstructure, a cross-sectional laser optical view of the surface-melted sample is shown in Fig. 2(a), which reveals the occurrence of two distinct zones, i.e., a melted zone and a heat-affected zone followed by the Mg-11Y-2.5Zn alloy substrate. It is apparent that the melted zone-heat-affected zone interface is crack/defect-free and well compatible with the heat-affected zone. Detailed microstructures in both the zones are shown in magnified views, as shown Fig. 2(b) to (d). The laser-melted zone extended up to an average depth of about 600 μm although there were minor variations in the laser-melted depth form place to place, consisted of two different morphologies, i.e., a 340 μm thick fine columnar dendrites followed by a 240 μm thick coarse columnar dendrites growing epitaxially from the liquid-semisolid interface. Laser surface melting is known to induce a rapid quenching effect to the shallow depth of surface layer that undergoes melting due to laser irradiation. Laser surface melting has produced fine microstructures (Fig. 2b, c), which resulted from high cooling rate of the surface. In the middle and the upper regions of the laser melt

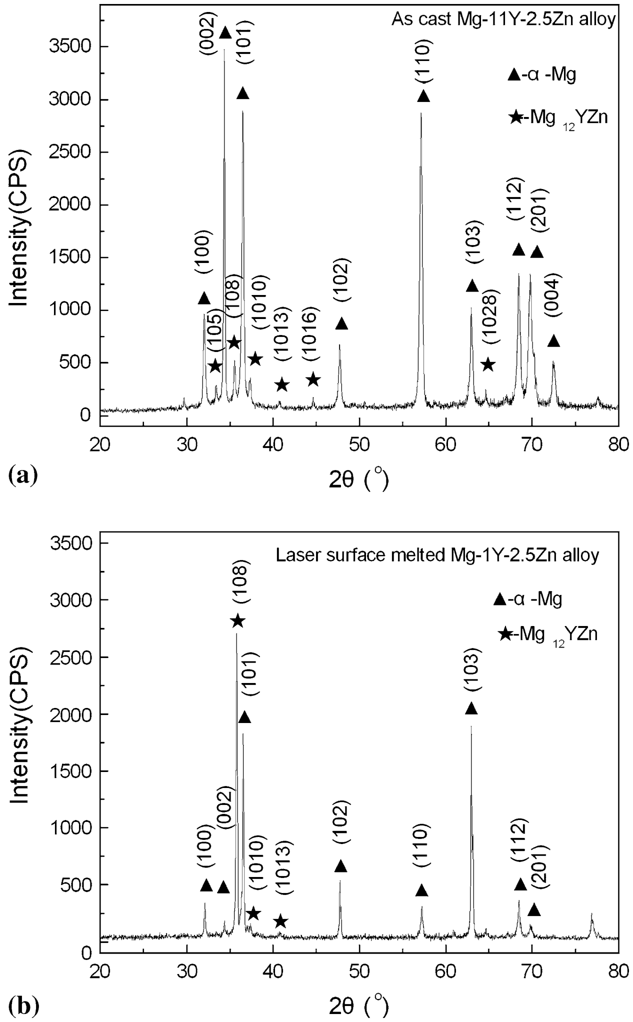

Fig. 1 The x-ray diffraction patterns of as-cast (a) and laser surface-melted (b) Mg-11Y-2.5Zn alloys

zone, the refined microstructure did not change the morphology due to the ratio of temperature gradient (G) and solidification rate (V). G/V was near constant according to the simulation results of solidifications in the literature (Ref 12, 13). Therefore, the microstructure was dependent on the cooling rates varying with the depth in melted zone. The solidification speed decreases with the increase of the depth, which makes columnar dendrites coarser in deeper depth. Since melting and solidification occur within a very short interaction time and remain confined to the top surface, the bulk underneath usually acts as an infinite heat sink without any noticeable change in microstructure. The fine α-Mg dendrite size was about 2 µm, the coarse α-Mg dendrite size was about 17 µm long and 5 µm wide, both were decorated with the discontinuous divorced eutectic $Mg_{12}ZnY$ phase at boundaries (see Fig. 2b, c). The discontinuous distributions of divorced eutectic intermetallic compound have been often observed in magnesium alloy such as AZ91 alloy and Mg-Zn-Y alloy (Ref 14, 15). The eutectic microstructure (α-Mg + divorced eutectic $Mg_{12}ZnY$) in Mg-11Y-2.5Zn alloy has been further confirmed by differential thermal analysis (DTA) of the laser-melted surface layer material, as shown in Fig. 3, in which an evident endothermic peak appears with an onset temperature of 543 °C, corresponding to melting of the eutectic, and an endothermic peak appears with an onset temperature of 614 °C, corresponding to melting of the α-Mg dendrites. Based on the kinetic undercooling theory in rapid solidification process (Ref 16, 17), the α-Mg cell propagated into the liquid from the original interface into the melted zone, while $Mg_{12}ZnY$ dendrite must nucleate first. Due to the much lower entropy of the fusion for α-Mg, the α-Mg cell had a much higher growth rate than did the $Mg_{12}ZnY$ dendrite. In a situation governed by kinetics, the faster growing phase predominated the microstructure. Therefore, α-Mg cells formed first, enriching Y and Zn in the surrounding regions, later $Mg_{12}ZnY$ eutectic phase formed from the melt at boundaries of the α-Mg dendrites. The amount of eutectic $Mg_{12}ZnY$ phase was increased as the solidification moved further to the melted zone. The heat-affected zone has morphology of semisolid microstructure with about 170 µm thickness and consisted of the coarse α-Mg dendrite with divorced eutectic $Mg_{12}ZnY$ phase at boundaries. It can be seen that the α-Mg dendrite is a little finer in heat-affected zone than in the substrate.

Refining of the microstructure in surface layer for the surface-melted alloy suggests a corresponding improvement in mechanical properties as shown in Fig. 4. Although, there is not much difference in hardness from the surface to the substrate, the hardness in different zones can still be divided into four minor levels in terms of the microstructure distribution, i.e., the highest hardness range of 77-83 HV for the fine dendritic microstructure, a moderate hardness value of 72-75 HV for the coarse dendritic microstructure, a comparable of 69-72 HV for heat-affected zone and the lowest hardness value of about 70 HV for the substrate.

3.2 Friction and Wear Behaviors

The coefficient of friction and wear rate for the untreated and surface-melted Mg-11Y-2.5Zn alloys as a function of load are shown in Fig. 5(a) and (b), respectively. The coefficients of friction for both the untreated and the surface-melted samples did not differ from each other greatly except at low load of 20 N. The applied load apparently had a significant effect on the coefficient of friction (see Fig. 5a) since the friction coefficient decreased with increasing load, decreased to about 0.4 as the load was increased to 80 N, and further decreased to be less than 0.3 under an applied load over 120 N, and finally to the lowest value of about 0.2 at 320 N for both untreated and surface-melted samples. Due to relatively low thermal strength, the friction characteristics of magnesium alloys are strongly influenced by changes in hardness or deformation resistance of Mg alloy surface as a result of the friction-induced temperature rise (Ref 9, 18). Our previous investigation of $Mg_{97}Zn_1Y_2$ alloy sliding against steel disk revealed that the worn surface temperature was estimated to be higher than 200 °C as load was over 40 N, and it is the thermal strength that play an important role in friction and wear characteristics because the yield strength decrease significantly at this stage (Ref 18). The crystalline structure of Mg alloys pins near their sliding surfaces flew to the sliding directions of disk because these parts of Mg alloys pins became soft enough with surface temperature rise. The part in which the shear resistance decreased and the crystalline structure was remarkably sheared to the frictional direction was named fluidity layer. The decrease in coefficient of friction for the untreated and

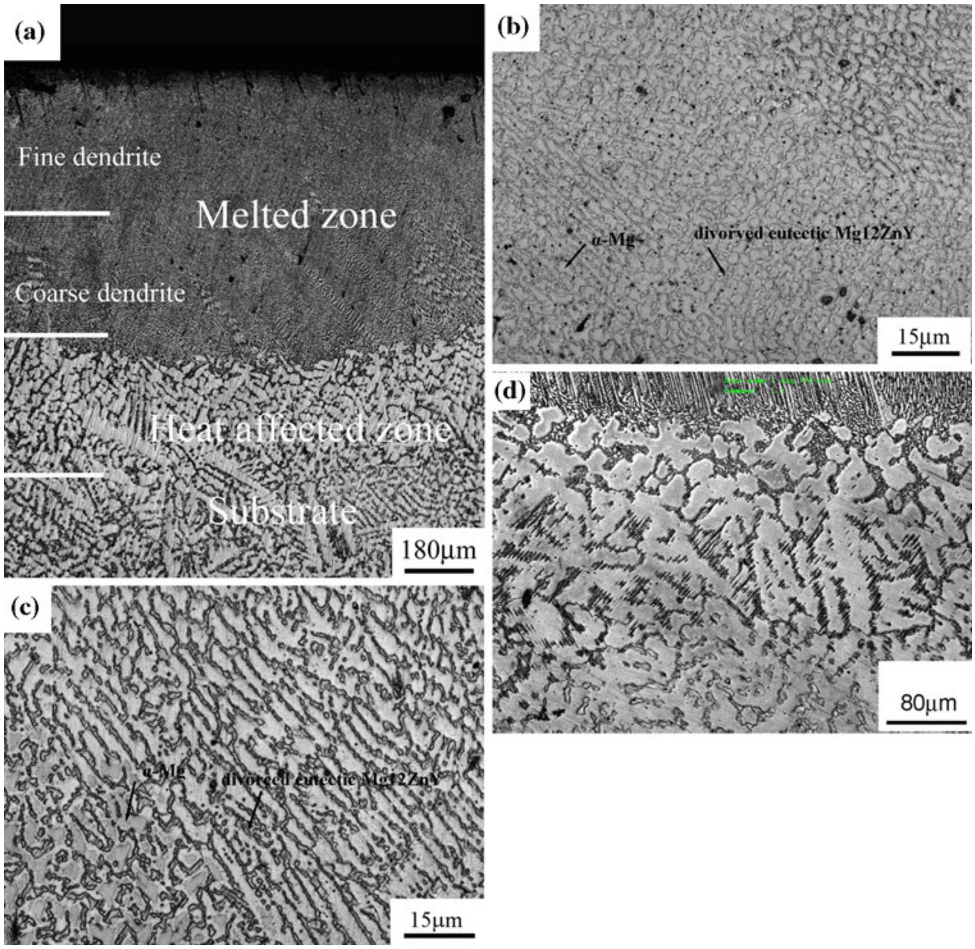

Fig. 2 Microstructures of laser surface-melted Mg-11Y-2.5Zn alloy: (a) the laser melted surface layer, (b) fine dendrite, (c) coarse dendrite, and (d) heat-affected zone

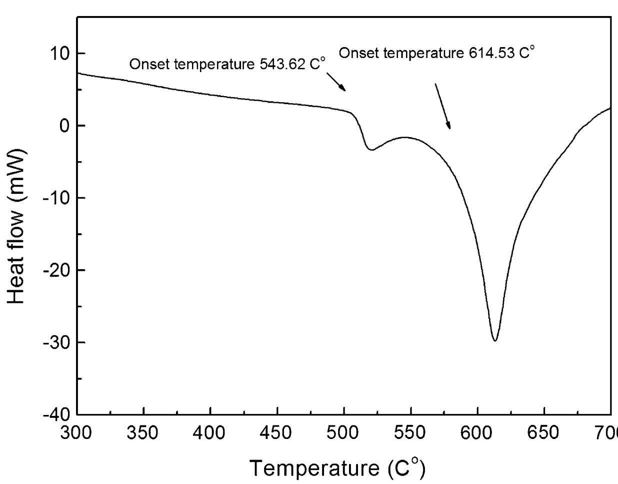

Fig. 3 DTA thermogram for the melted layer material on Mg-11Y-2.5Zn alloy substrate

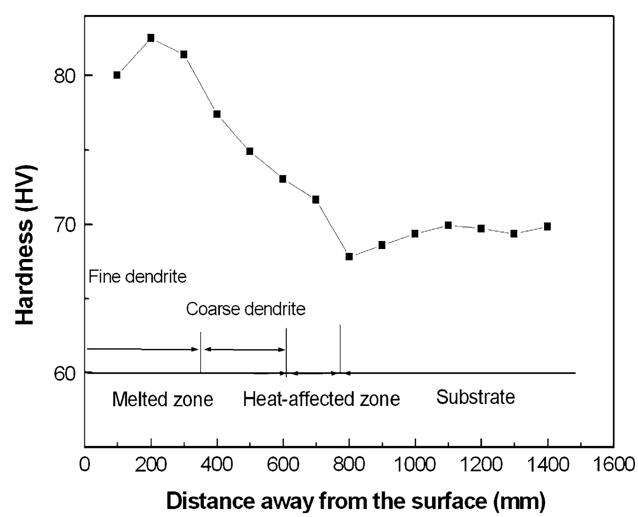

Fig. 4 Hardness profile of laser surface-melted Mg-11Y-2.5Zn alloy

surface-melted Mg-11Y-2.5Zn alloys decreased with the increase of applied load is attributed to the surface softening induced by friction heating, and it is confirmed by the evident plastic deformation on the cross-sectional micrographs of the pin surfaces as shown in Fig. 6(a) and (b). The reason why coefficient of the untreated and laser surface-melted Mg-11Y-2.5Zn alloys did not differ from each other very much could be due to three aspects: first, the limited increment of hardness in melted zone (7-13 HV) for laser surface-melted Mg-11Y-2.5Zn alloys at room temperature may decrease or

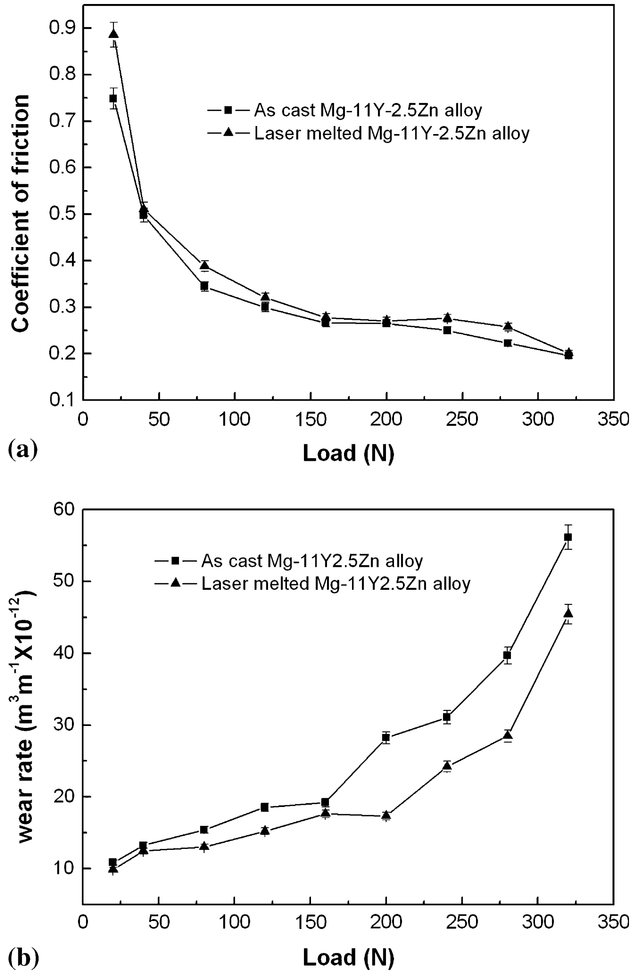

Fig. 5 The variation in coefficient of friction (a) and wear rate (b) with load for as-cast and laser surface-melted Mg-11Y-2.5Zn alloys

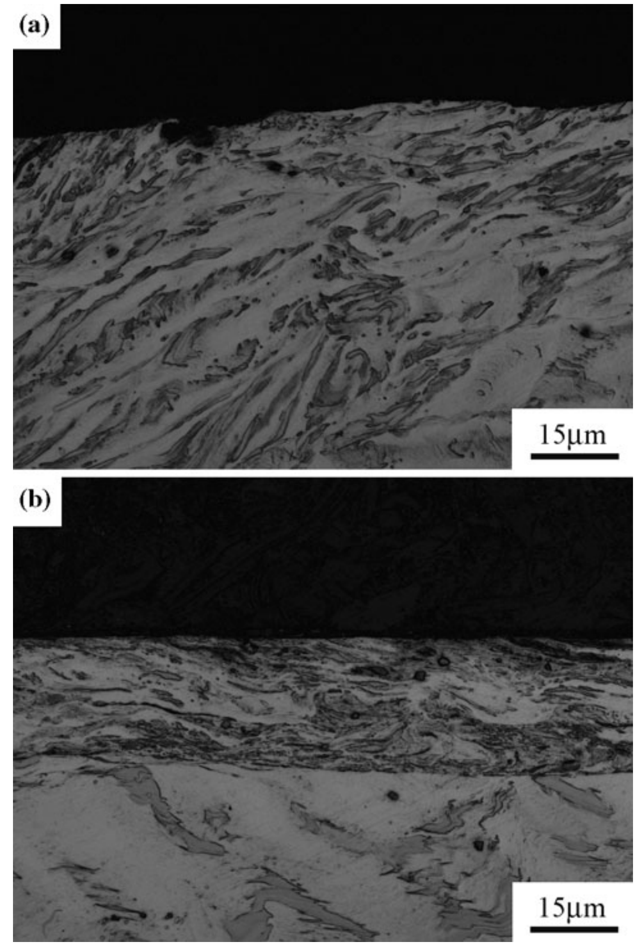

Fig. 6 Microstructures of plastic deformation of subsurface for untreated (a) and laser surface-melted (b) pins subjected to 160 N

finally disappear as compared to the untreated alloy when the worn surface softens at applied load over 40 N. Second, the plastically deformed zone extends beyond the surface melted zone to the substrate (see Fig. 6a), therefore, the effect of the surface-melted zone on the coefficient of friction is limited. Third, the accumulation of debris on the wear track could also shadow the difference in coefficient of friction between the untreated and the laser surface-melted Mg-11Y-2.5Zn alloys. A similar phenomenon was reported in investigation on laser surface melting of AM50 magnesium alloy, in which the friction coefficient curve of the laser surface-melted specimen was similar to that of the untreated specimen even though the laser surface-melted AM50 magnesium alloy was 25-30 HV higher than the untreated one (Ref 19).

The surface melting treatment has a positive effect on wear rate (Fig. 5b). It is noticeable that the surface-melted alloy presents a better wear resistance when compared with the untreated one in the applied load range of 20-320 N. The wear rate of the surface-melted alloy increases gradually until 200 N and then goes up dramatically, while the wear rate of the untreated alloy increases slightly faster than laser treated alloy until 160 N and then also increases rapidly. It is noticeable that the wear rates versus load for untreated and laser surface-melted alloys show almost the same nature (i.e., slopes of the wear rate curves are almost same), which implies the same wear mechanisms in operation in different load ranges for the untreated and laser surface-melted alloys as discussed in Section 3.3.

In order to understand the effect of microstructure in melted zone on the wear rate, the volume loss of specimen is transformed into depth loss as shown in Fig. 7. In consideration of the material previously removed off from the wear specimens, the wear depth increased gradually and remains within the fine dendritic microstructure region as the load was less than 200 N, while beyond that load the wear depth increased dramatically and reached coarse dendritic microstructure region. Even though this result cannot clarify the difference in wear resistance between the fine and the coarse dendritic microstructures, it still indicates that the fine microstructure exhibits better wear resistance as compared with as-cast microstructure, and can delay the transformation from mild wear to severe wear as compared with the untreated alloy. This conclusion can be drawn on the basis of observation of worn surface where abrasive wear and plastic deformation are main wear mechanisms for the studied alloy, improvement in both hardness and refinement of microstructure in the melted layer bring about difficulty in plastic deformation and delamination is consequently beneficial to the decrease in wear rate. The surface cracks originated from coarse $Mg_{12}ZnY$ compound can be observed in the cross-sectional micrograph of worn surface for the untreated alloy (Fig. 8), which finally lead to quick delamination. As the grain size and hardness in the heat-affected zone for the laser-treated alloy were analogous to those of the untreated alloy, the wear resistance of the heat-affected zone is considered not to be much better than the untreated alloy.

3.3 Wear Mode

SEM photographs of the worn surfaces of the untreated and laser-melted Mg-11Y-2.5Zn alloys at different loads are shown in Fig. 9 and 10, respectively. In the case of untreated Mg-11Y-2.5Zn alloy, at low load of 20 N, the worn surface was covered with deep furrows parallel to the sliding direction, as shown in Fig. 9(a). This is typical feature associated with abrasive wear, in which hard asperities on the steel counterface, or hard particles in between the pin and the disk, plough or cut into the pin, causing wear by removal of small fragment or ribbon-like strips of material. In addition to this, repetitive plastic grooving was also associated with the fatigue and fracture of inter-grove ridges. The edge fracture process resulted in the formation of thin shard of wear debris. As the load was increased from 80 to 160 N, the furrows were much deeper and the cracks at an angle of 45° or roughly perpendicular to the sliding direction can be observed (see Fig. 9b), which is generally associated with delamination, indicating abrasion and delamination were the main wear mechanisms. At this stage, the delamination

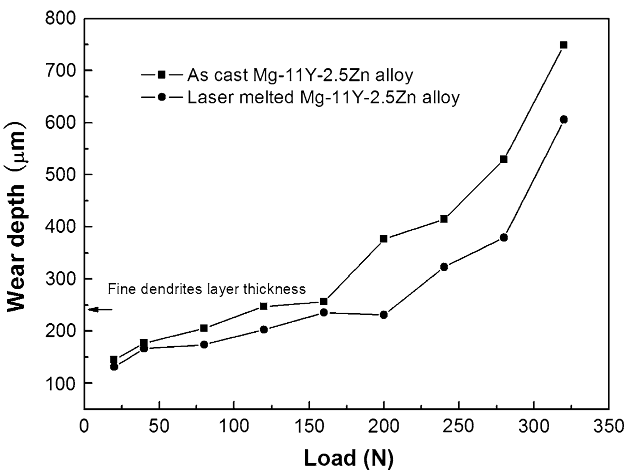

Fig. 7 The variation in wear depth with load for as-cast and laser surface-melted Mg-11Y-2.5Zn alloys

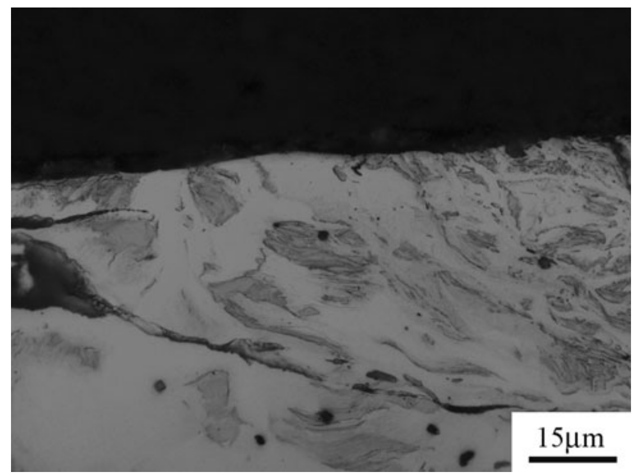

Fig. 8 Cracks in the plastic deformation zone of the untreated pin subjected to 160 N

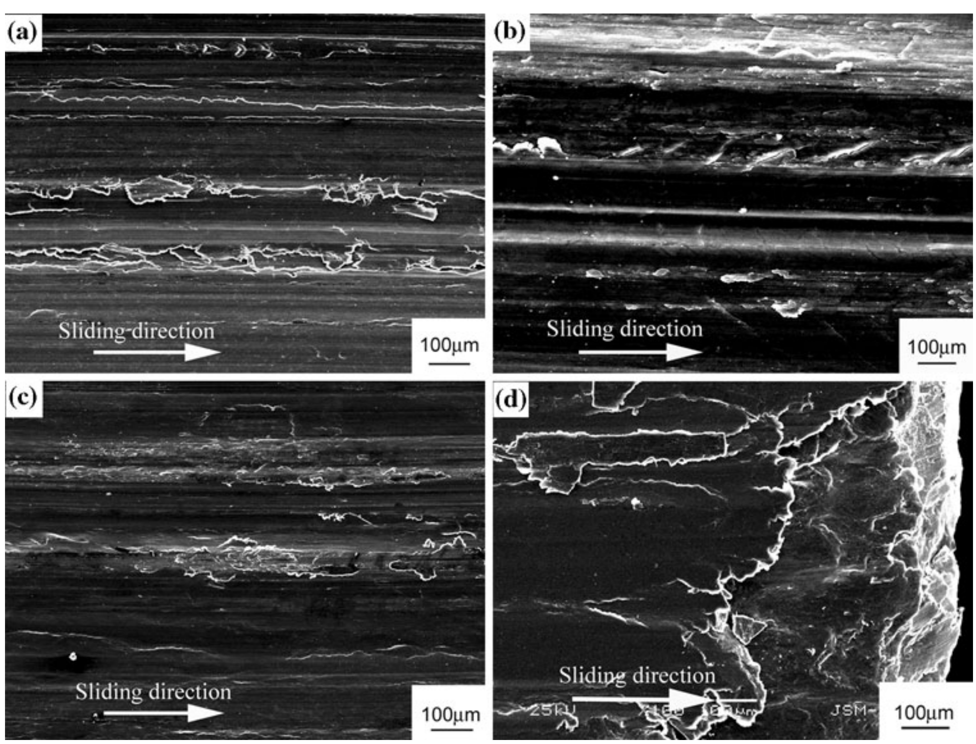

Fig. 9 SEM micrographs of worn surfaces of as-cast alloy at different applied loads: (a) 20 N, (b) 80 N, (c) 200 N, and (d) 320 N

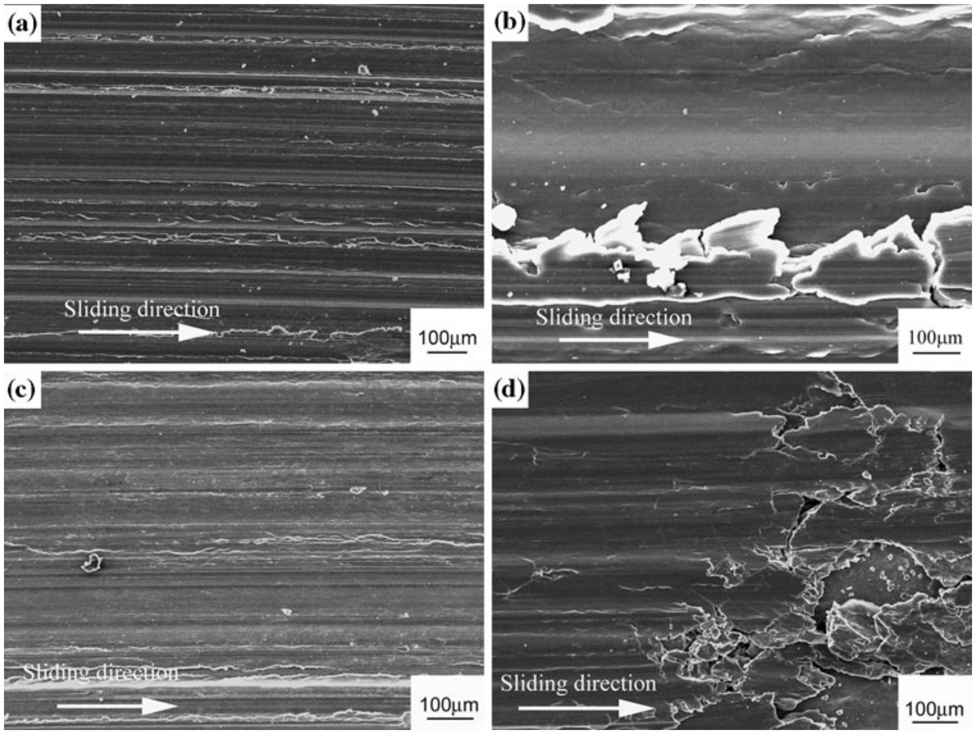

Fig. 10 SEM micrographs of worn surfaces of laser surface-melted alloy at different applied loads: (a) 20 N, (b) 80 N, (c) 280 N, and (d) 320 N

often arises from the subsurface cracks initiated from the coarse $Mg_{12}ZnY$ compound particles for untreated alloy. As the load was further increased to 200-240 N, the plastic deformation of the surface became more evident so that the surface became a little smooth, more materials was extruded outwards the sample edge besides a few craters on the worn surface (Fig. 9c). Under the most severe sliding condition of 280-320 N, gross plastic deformation of the pin surface occurs and material is extruded from the interface before re-solidifying around the periphery of the pin (Fig. 9d). The pin surface left behind also appears much smoother than those worn under other sliding conditions. These observations are associated with softening and melting of the material caused by frictional heating at the sliding interface.

When contacting solids slide, work is done against friction. Almost all the frictional work appears as heat, generated at or very close to the surface at which the two solids meet (Ref 20). The temperature raise at the worn surface has an impact on wear behavior by changing microstructure and mechanical properties in the surface layer of the pin. The local increase in temperature influences both the friction and the wear rate. Magnesium alloys are one of the most sensitive materials to the temperature since their mechanical properties vary a lot with increasing temperature due to their low melting point of intermetallic phases, which can readily soften at elevated temperatures. In the low and moderate load range, it is the thermal strength that plays a dominant role in wear properties. With increasing the applied load, the temperature on the worn surface increased gradually, therefore, the material on the surface became soft, giving rise to a decrease in coefficient of friction and an increase in wear rate. As the temperature on the surface was near or above the melting of the material, the worn surface became so softer that a large amount of material was extruded to the pin edge, resulting in a remarkable increase in wear rate. The coefficient of friction was correspondingly at the lowest level due to the lubricating effect of the melted metal. Similar findings of material softening and melting were previously reported in pin-on-disk wear tests of AZ91and Mg97Zn1Y2 magnesium alloys (Ref 9, 18).

For the laser surface-melted Mg-11Y-2.5Zn alloy, the refining of the microstructure induced by laser treatment improves the properties of the surface layer; the wear resistance was thus better than that of the untreated alloy. At low load of 20 N, grooves with plastic deformation concluded the abrasion was the wear mechanism (Fig. 10a). With the load was increased to 80 N, a series of cracks perpendicular to the sliding direction were formed, indicating abrasion and delamination were the main wear mechanisms (Fig. 10b). However, the distribution of cracks on laser surface-melted alloy was not as dense as it was on the worn surface of the untreated alloy; this could be due to the fine $Mg_{12}ZnY$ compound particles formed by non-equilibrium solidification process by laser surface melting. The fine compound particles cannot induce high stress concentration, and hence reduce the probability of crack initiation and lessen the delamination. With increasing load, these mechanisms remained the same until 200 N. In the load range of 240-280 N, thermal softening was an important wear mechanism, for the surface became much smoother (see Fig. 10c) and the extruded edges of specimens were evident. At the load 320 N, the local temperature of the contact surface exceeded the melting temperature of the alloy. The molten material spread out of the contact surface in the sliding direction as well as by moving sideways. During the sliding wear, the solidified material formed thin layers, and new layers were continuously generated over the previously formed layers as the previously molten material extruded out of the contact surface (Fig. 10d).

4. Conclusions

Surface melting of Mg-11Y-2.5Zn alloy was performed with a 6.0 kW CO_2 laser. Two distinct zones including the melted zone and heat-affected zone were formed sequentially near the surface of Mg-11Y-2.5Zn alloy; laser surface melting refines the α-Mg dendrites and $Mg_{12}ZnY$ compound particles, and increases the hardness in the melted zone. The wear rate in sliding can be decreased by laser surface melting treatment; the fine microstructure in laser-melt zone exhibits good wear resistance as compared with the as-cast material in a load range of 20-200 N. The wear mode varies from abrasion and delamination at both low and mediate loads to the thermal softening and melting at high load.

Acknowledgment

The authors thank the Project 985-automotive engineering of Jilin University and Technology Development Program of Jilin Province (No. 20080309).

References

1. A.A. Luo, Recent Magnesium Alloy Development for Automotive Powertrain Applications, *Mater. Sci. Forum*, 2003, **419**, p 57–65
2. M.M. Avedesian and H. Baker, *Magnesium and Magnesium Alloys-ASM Specialty Handbook*, ASM International, Materials Park, OH, 1999, p 87
3. Y. Kawamura, K. Hayashi, A. Inoue, and T. Masumoto, Rapidly Solidified Powder Metallurgy $Mg_{97}Zn_1Y_2$ Alloys with Excellent Tensile Yield Strength Above 600 MPa, *Mater. Trans. JIM*, 2001, **42**, p 1172–1176
4. A. Inoue, Y. Kawamura, M. Matsusita, K. Yhayashi, and J. Koike, Novel Hexagonal Structure and Ultrahigh Strength of Magnesium Solid Solution in the Mg-Zn-Y System, *J. Mater. Res.*, 2001, **16**, p 1894–1990
5. M. Matsuda, S. Ii, Y. Kawamura, Y. Ikuhara, and M. Nishida, Interaction Between Long Periods Stacking Order Phase and Deformation Twin in Rapidly Solidified $Mg_{97}Zn_1Y_2$ Alloy, *Mater. Sci. Eng. A*, 2004, **386**, p 447–452
6. Joint Committee on Powder Diffraction Standards, Powder Diffraction File, Inorganic Phases Card 36-1273
7. S.C. Sharma, B. Anand, and M. Krishna, Evaluation of Sliding Wear Behavior of Feldspar Particle-Reinforced Magnesium Alloy Composites, *Wear*, 2000, **241**, p 33–40
8. C.Y.H. Lim, S.C. Lim, and M. Gupta, Wear Behaviour of SiC_p-Reinforced Magnesium Matrix Composites, *Wear*, 2003, **255**, p 629–637
9. H. Chen and A.T. Alpas, Sliding Wear Map for the Magnesium Alloy Mg-9Al-0.9Zn (AZ91), *Wear*, 2000, **246**, p 106–116
10. J.D. Majumdar, R. Galun, B.L. Mordike, and I. Manna, Effect of Laser Surface Melting on Corrosion and Wear Resistance of a Commercial Magnesium Alloy, *Mater. Sci. Eng. A*, 2003, **361**, p 119–129
11. G. Abbas, L. Li, U. Ghazanfar, and Z. Liu, Effect of High Power Diode Laser Surface Melting On Wear Resistance of Magnesium Alloy, *Wear*, 2006, **260**, p 175–180
12. S.Y. Liu, J.D. Hu, Y. Yang, Z.x. Guo, and H.Y. Wang, Microstructure Analysis of Magnesium Melted by Laser Irradiation, *Appl. Surf. Sci.*, 2005, **252**, p 1723–1731
13. A. Basu, A.N. Samant, S.P. Harimkar, J. Dutta Majamdar, I. Manna, and N.B. Dahotre, Laser Surface Coating of Fe-Cr-Mo-Y-B-C Bulk Metallic Glass Composition on AISI, 4140 Steel, *Surf. Coat. Technol.*, 2008, **202**, p 2623–2631
14. A. Srinivasan, J. Swaminathan, M.K. Gunjan, and U.T.S. Pillai, Effect of Intermetallic Phases on the Creep Behavior of AZ91 Magnesium Alloy, *Mater. Sci. Eng. A*, 2010, **527**, p 1395–1403
15. A. Muller, G. Garces, P. Perez, and P. Adeva, Grain Refinement of Mg-Zn-Y Alloy Reinforced by an Icosahedral Quasicrystalline Phase by Severe Hot Rolling, *J. Alloy Compd.*, 2007, **443**, p 1–5
16. D.M. Stefanescu, R. Ruxanda, Fundamentals of Solidification, 9th ed., Vol 9, ASM Handbook, ASM International, Materials Park, OH, 2004
17. L.E. Greenwald, E.M. Breinan, and B.H. Kear, *Laser-Solid Interaction and Laser Processing*, S.D. Ferris, H.J. Leamy, and J.M. Poate, Ed., American Institute of Physics, New York, 1978,
18. J. An, R.G. Li, and Y. Lu, Dry sliding Behavior of Magnesium Alloys, *Wear*, 2008, **265**, p 97–104
19. Y.K. Zhang, J.F. Chen, W.N. Lei, and R.J. Xv, Effect of Laser Surface Melting on Friction and Wear Behavior of AM50 Magnesium Alloy, *Surf. Coat. Technol.*, 2008, **202**, p 3175–3179
20. M.F. Ashby, J. Abulawi, and H.S. Kong, Temperature Maps for Frictional Heating in Dry Sliding, *Tribol. Trans*, 1991, **34**, p 577–587